



Published in final edited form as:

Nat Photonics. 2011 October 1; 5(10): 591–597. doi:10.1038/nphoton.2011.206.

Optofluidic Microsystems for Chemical and Biological Analysis

Xudong Fan¹ and Ian M. White²

¹Biomedical Engineering Department, University of Michigan, Ann Arbor, MI 48109, USA

²Fischell Department of Bioengineering, University of Maryland, College Park, MD 20742, USA

Abstract

Optofluidics – the synergistic integration of photonics and microfluidics – has recently emerged as a new analytical field that provides a number of unique characteristics for enhanced sensing performance and simplification of microsystems. In this review, we describe various optofluidic architectures developed in the past five years, emphasize the mechanisms by which optofluidics enhances bio/chemical analysis capabilities, including sensing and the precise control of biological micro/nanoparticles, and envision new research directions to which optofluidics leads.

Optics has long been used to analyze bio/chemical samples. In recent decades, optical sensing systems have evolved from bulk systems, such as flow cytometers and microplate readers, to microdevices, such as waveguides and resonators on a chip. In parallel to this development, microfluidics has emerged, which enables small volume sample handling and delivery, and can perform a number of automated functions, such as particle sorting and separation, cell culture, and concentration gradient formation. The synergy of the recent technological advances in both photonics and microfluidics leads to optofluidics, where photonic and microfluidic architectures are organically integrated to enhance each entity's function and performance.

Since its debut few years ago, optofluidics has quickly found a broad range of applications, as described in the accompanying review articles by Erickson, *et al.*, and Schmidt and Hawkins, in this *Nature Photonics* issue, as well as a few review articles and books published recently^{1–4}. In particular, optofluidics is well suited for bio/chemical detection and analysis in extremely small detection volumes (fL–nL) due to the complementary integration of the sample preparation and delivery with the analytical mechanism. As illustrated by many examples presented in this article, microfluidics is not merely an add-on accessory to an optofluidic device, but rather, an integral part of it^{5–8}. Such integration creates a number of unique characteristics that can be leveraged for bio/chemical analysis. Many optical properties, such as refractive index (RI), fluorescence, Raman scattering, absorption and polarization, can be exploited individually or in combination to generate the sensing signal. Detection can be carried out in either the linear^{5–8} or non-linear optical regime^{9–11}. Adaptation of traditional analytical chemistry technologies such as chromatography and electrophoresis to optofluidic devices further increases their functionalities in bio/chemical analysis^{12–16}. Additionally, optofluidic microsystems can employ optical forces in concert with microfluidics to trap and manipulate targets to enhance the analytical capabilities¹⁷.

This article overviews the state-of-the-art of optofluidic architectures in bio/chemical analysis. Based on the analytical mechanisms, it is grouped into four sections, *i.e.*, RI

Contact information X. Fan: xsfan@umich.edu I. M. White: ianwhite@umd.edu.

Author contributions X.F. and I.M.W. contributed equally to this article.

detection, fluorescence detection, SERS detection, and optical trapping and manipulation. Emphasis is given on how optofluidics can enhance the overall analytical performance. At the conclusion, potential advancement of optofluidics in bio/chemical analysis is discussed.

Optofluidic sensors with RI-based detection

RI detection has been one of the most popular bio/chemical analysis methods used in optofluidic sensors. It is primarily distinguished as a label-free sensing technique, as opposed to fluorescence labeling. Optofluidic RI sensors measure RI changes of bulk solution due to the homogeneous presence of analytes, or near the sensor surface due to the attachment of analytes, as those analytes typically have different RI (or excess polarizability) from the background solution. RI detection is particularly attractive for optofluidic sensors having extremely low detection volumes, as the RI signal scales with the analyte bulk concentration or surface density, rather than the total number of molecules. In many optofluidic RI sensors, the electric field can be confined within a small volume (fL-nL), thus enabling the detection of molecules of ultra-low quantity. To date, various optofluidic architectures, including metallic nanohole array based plasmonics^{6, 18–22} (see Fig. 2a), photonic crystals (PCs) and photonic crystal fibers (PCFs)^{7, 23–32} (see Fig. 2b and c) as well as interferometric structures, such as ring resonators^{33–38} (see Fig. 2d and e), Mach-Zehnder interferometers^{39, 40} and Fabry-Pérot (FP) cavities^{8, 41–43} (see Fig. 2f), have been explored to maximize light-analyte interaction while satisfying other requirements in bio/chemical analysis.

Plasmonic-, PC-, and PCF-based optofluidic RI sensors are mainly based on periodic metallic or dielectric structures to confine and guide the light (see Fig. 2a–c). The voids in these structures are inherently excellent microfluidic channels to fill with liquid samples for bio/chemical sensing. The surface detection sensitivity on the order of 1 nm/nm (*i.e.*, 1 nm spectral shift per nanometer of molecular attachment, where 1 nm increase in height on the sensor surface corresponds to approximately 1 ng/mm² of biomolecular attachment^{44, 45}), has been demonstrated^{18, 25, 28}. Due to the extremely small effective sensing area used, biomolecules of only fg to sub-fg in mass can potentially be detected^{25, 27}. Unfortunately, in practice such unprecedented detection capability is often plagued by the rudimentary sample delivery system that is unable to deliver analytes selectively to the place where the light-matter interaction is the strongest.

Recently, a few optofluidic techniques have been reported, in which the photonic device inherently integrates with a microfluidic channel for simple and repeatable sample delivery. The optofluidic ring resonator (OFRR) represents an example of this optofluidic advancement^{33–38} (see Fig. 2c and d). OFRRs have been realized using thin-walled cylindrical capillaries, self-assembled tubes on-chip, glass micro-bubbles, and antiresonant reflecting optical waveguides (ARROWS). They retain the original excellent ring resonator sensing capability⁴⁶ while forming integrated microfluidic structures as well. Detection of various chemical and biological samples ranging from small molecules such as biotin to large species such as viral particles has been demonstrated^{36, 47}. The sensitivity is about 570 nm/RIU (refractive index units) and 0.02 nm/nm for bulk RI detection and surface detection, respectively with the corresponding detection limit of 10⁻⁷ RIU and 1 pg/mm²³⁶. Similar to the OFRR, in an optofluidic FP cavity sensor, the liquid channel is also part of the sensing cavity^{41–43}. FP sensors probe the entire sample volume, enabling “whole body” detection, which is particularly useful for cell detection (see Fig. 1f). Using this method, Shao, *et al.*, differentiated lymphoma cells from normal lymphocytes⁴².

Another problem faced by photonic sensors, even when integrated with a microfluidic sample delivery system, is the mass transport of the target molecules to the sensor surface.

Very recently, an optofluidic “flow-through” strategy in replacement of “flow-over” has been explored in several designs to mitigate the slow mass transport issues encountered by most optical sensors. This optofluidic technique integrates nanofluidic channels through the optical sensing structure such that the entire sample interacts directly with the sensitive surface. Mass transport to the sensing surface is almost entirely convective instead of diffusive, which results in a stronger signal in significantly less time. Plasmonic nanofluidic sensors and PC nanofluidic sensors fabricated by photolithography consist of arrays of nanoholes, as shown in Fig. 1g^{6, 7, 21, 22}. The wafer substrate is back-etched so that the liquid can be driven through the thin (~100 nm) holey metal or dielectric membrane. Bulk RI sensitivity and surface attachment sensitivity of 600 RIU/nm and 2 nm/nm have been achieved^{6, 21}. 14-fold and 6-fold enhancement in the mass transport rate over the established flow-over method have been demonstrated for bulk solution and for small molecules, respectively^{6, 21} (see Fig. 1g). Guo, *et al.*, developed another flow-through design illustrated in Fig. 1h⁸. Thousands of sub-micron sized holes in a capillary form nanofluidic channels as well as part of an FP cavity. This nanofluidic capillary is similar to the nanoporous sensor^{48, 49}, but has well-defined flow-through holes fabricated through the drawing method. Therefore, it has high surface mass sensitivity (10–20 nm/nm) resulting from the large surface-to-volume ratio, while achieving much more efficient sample delivery.

In addition to working as a stand-alone sensor, optofluidic RI sensors have been incorporated with traditional analytical chemistry technologies, such as chromatography and electrophoresis, for enhanced sample analysis capabilities. Such marriage often leads to a device acting as separation column and on-column detector, which enables the real-time detection of the analytes being separated and minimizes connections used in microfluidics. Two examples of such on-column optofluidic RI sensors have been demonstrated by Wang, *et al.*, and Zhu, *et al.*, respectively, based on back-scattering interferometry¹² and thin-walled capillary OFRR¹³, both of which measure the bulk RI change at any pre-determined location along the column when analytes pass through the detection location.

Fluorescence-based optofluidic sensors

While label-free sensing is advantageous because of the reduced number of biosensing steps, a number of applications remain in which fluorescence-based sensing is of value. One of the major research focuses in optofluidic fluorescence detection is to improve the confinement and guiding of light in low index buffer solution (composed mainly of water) where analytes reside, which enhances the light-fluorophore interaction and fluorescence collection efficiency for a better detection limit. To this end, various optofluidic architectures have been developed, including (1) liquid core waveguides using low index cladding materials, such as Teflon^{50, 51} and nanoporous materials^{52, 53} to guide the light through total internal reflection; (2) PC structures that enhance the fluorescence signal and provide better fluorescence collection efficiency^{54–58}; and (3) slot waveguides that confine both liquid and light within the same sub-micron-sized channel⁵⁹. Among those, the ARROW (discussed previously) is one of the most promising optofluidic sensing structures to achieve confinement and guiding of light and liquid^{5, 38, 60–64}. Used in fluorescence detection^{5, 60, 61, 64}, the ARROW is able to achieve a sub-pL excitation or detection volume, thus allowing for sensitive detection down to extremely low analyte quantity. Schmidt, Hawkins, and co-workers demonstrated detection of a single molecule and a single particle in free solution directly or through fluorescence correlation spectroscopy^{5, 60, 64}. Recently, the same team implemented dual color fluorescence cross-correlation spectroscopy to detect particle co-localization and, in combination with fluorescence resonance energy transfer (FRET), DNA binding and denaturation⁶¹. These achievements may bode well for the eventual replacement of conventional bulky and expensive fluorescence microscopes with inexpensive optofluidic devices for rapid and *in-situ* bio/chemical analysis.

The optofluidic laser is another versatile and promising platform for bio/chemical analysis. It usually consists of a microfluidic laser cavity to provide the optical feedback and a fluorophore solution as the gain medium, which enables intra-cavity detection. In contrast to other optofluidic fluorescence sensors discussed previously, the optofluidic laser sensor relies on stimulated emission as the sensing signal and therefore is highly sensitive to any small perturbations to the laser cavity or the gain medium. While presently most effort has been focused on the development of the laser itself⁶⁵, a few intra-cavity sensing demonstrations have been reported to reveal the vast capabilities of the optofluidic laser. Based on a simple optofluidic FP-cavity-based dye laser, Galas, *et al.*, carried out sensitive intra-cavity absorption measurements using the laser emission change⁹. More recently, Sun, *et al.*, employed the OFRR laser in conjunction with FRET for sensitive DNA detection¹⁰. The hybridization of the DNA probe and target causes FRET between the donor and acceptor labeled respectively on the DNA samples, leading to drastic reduction in the initial lasing emission from the donor and the emergence of the acceptor lasing and hence a significantly increased sensing signal in comparison with that in the conventional FRET method. Moving a step forward, the same group recently reported highly selective single nucleotide polymorphism detection using the OFRR and molecular beacon (MB) approach¹¹. In the presence of the target DNA, the OFRR is operated above the lasing threshold and thus generates strong lasing emission. In contrast, with the single-base mismatched DNA, the OFRR is below the lasing threshold and only virtually negligible fluorescence background is observed. Through this analog-to-digital-conversion-like detection, over two orders of magnitude enhancement in the discrimination ratio between the target and single-base mismatched DNA has been achieved.

Optofluidic SERS-based analysis

Surface enhanced Raman spectroscopy (SERS) may have the potential to provide the advantages of the simplicity of label-free analysis and the low detection limits of fluorescence-based detection, as well as the molecular-specific Raman spectrum for analyte identification. SERS utilizes the well-understood electromagnetic enhancement provided by metal nanostructures⁶⁶ as well as a chemical enhancement due to metal-molecule interactions, which is not yet well understood^{67, 68}, to achieve several orders of magnitude increase in the Raman scattering cross section. In fact, SERS has been utilized to observe Raman scattering from single molecules^{69, 70}. While it has been nearly 35 years since the first demonstrations of SERS^{71, 72}, the practical applications of this powerful technique are still quite limited today.

One path to increase the practical use of SERS is to integrate the detection into a microfluidic system along with other functions. Two common implementations are (1) to pass the sample through a channel in a metal nanoparticle colloid solution and (2) to integrate a metal nanostructured surface at the bottom of a microfluidic channel. In general, however, conducting SERS measurements within a microfluidic environment can be detrimental to the detection limit because of the reduced number of SERS-active sites in method (1) and the low mass transport of analyte molecules to the SERS-active surface in method (2). Optofluidic SERS approaches have emerged in recent years that compensate for these shortcomings by increasing the number of target analyte molecules that are excited by the excitation source or that interact with SERS-active surfaces, which, as a result, improves the SERS performance.

One optofluidic approach to accomplish this is to utilize photonic geometries that extend the detection volume, thus including a higher number of analyte molecules and SERS-active sites. For example, PCFs (see Fig. 1c) utilize the holey core or cladding as a microfluidic channel; the excitation light and the Raman scattered photons propagate along with the

sample inside the PCF, and thus the detection volume extends for the length of the PCF. Yang, *et al.*, utilized the hollow core of the PCF as the microfluidic channel⁷³, while Khaing Oo, *et al.*, utilized a holey cladding as the microfluidic channel⁷⁴. In each case, the reported detection limit for Rhodamine 6G (R6G) was 100 pM, which is significantly improved as compared to reported detection limits using the conventional microfluidic SERS approached described above. This optofluidic SERS concept was translated to an on-chip implementation by Measor, *et al.*⁷⁵ based on the ARROW structure discussed previously. This on-chip implementation combines the optofluidic SERS enhancement with the ability to integrate other on-chip functions with SERS detection.

Another optofluidic approach is to leverage micro- and nano-fluidic techniques to increase the performance and utility of SERS by concentrating analytes or analyte-nanoparticle aggregates into the detection volume, which eliminates the reliance on diffusion to carry targets into the detection volume. This can be done passively by designing geometries that perform the concentration, as achieved by Wang, *et al.*, who constructed a device that utilized a 40 nm high channel between the inlet and outlet⁷⁶. Metal nanoparticles were trapped at the inlet to the nanochannel, forming a high density of SERS-active sites. Using a similar concept, Park, *et al.*, reported the detection of a Cy3-labeled DNA sequence marker for Dengue virus using SERS⁷⁷. In this case, the authors formed nanofluidic channels as small as 60 nm using elastomeric collapse in polydimethylsiloxane (PDMS) at the inlet. In another example of nanofluidics for SERS enhancement, Liu, *et al.*, utilized a nanoporous polymer monolith within a microfluidic channel to trap and concentrate silver nanoparticles in a 3-D matrix⁷⁸. As compared to a conventional 2-D SERS active surface, this design creates a 3-D SERS-active matrix, eliminating the need for diffusion of analyte molecules to the surface.

Active microfluidic techniques have also been implemented in optofluidic SERS approaches to concentrate the nanoparticles, the analyte molecules, or both, prior to SERS detection. Huh, *et al.*, utilized electrokinetic forces within a microfluidic chamber to attract metal nanoparticles as a method of concentrating the nanoparticle-target conjugates into the SERS detection volume⁷⁹. Electrokinetic forces can also be used for concentration of the analyte at a SERS-active surface. Cho, *et al.*, created a microfluidic channel on top of a SERS-active surface and located an electrode at the top of the channel⁸⁰. With a potential applied between the electrode and the metal-nanostructured surface, the analyte molecules are driven to the SERS-active surface, and thus all of the analyte in the entire sample volume was concentrated at the detection zone (Fig. 2a), again avoiding the need to rely on diffusion for interaction between the SERS-active surfaces and the analyte. With the tremendous enhancement created by this microfluidic technique, the authors detected 10 fM adenine.

In addition to increasing the number of analyte molecules that interact with SERS-active sites in the detection volume, another optofluidic approach that holds great potential for increasing the performance of SERS is to utilize optofluidic resonators for SERS excitation within a micro- or nano-fluidic environment. Optical resonators possess enhanced field intensities at the surface, which can act as high-power excitation sources for SERS. Although there are a few reports of optical resonators as sources of SERS excitation^{81, 82}, this optofluidic design concept remains for the most part uncultivated today. Furthermore, building upon some of the developments in optofluidics, there is a great potential to integrate the optofluidic resonator approach with the micro- or nano-fluidic concentration approaches outlined above, which may result in extraordinary SERS performance.

In addition to increasing the detection capabilities, optofluidics is also creating unique applications of SERS that have not been possible before. For example, building upon the PDMS nanochannels described above, Choi, *et al.*, have reported the selective detection of

protein aggregates, which play a role in a number of diseases, including Alzheimer's⁸³. After nanoparticles form a concentrated network at the inlet of the nanochannel, aggregated proteins are trapped in the detection zone and thus produce a detected SERS signal, while monomer proteins migrate through the detection zone and are not detected (Fig. 2b). Another application of optofluidic SERS recently demonstrated by Lee, *et al.*, is to incorporate an on-column SERS-based detector with chromatographic separation of metal ions¹⁶. The inside surface of the capillary, which is coated with carboxylated gold nanoparticles, serves as the separation medium (due to selective adsorption properties of the metal ions) and also as the SERS-active surface. This eliminates the need for a post-separation detection mechanism, such as mass spectrometry. It is expected that applications of SERS will continue to emerge from other new advancements in optofluidics, including the introduction of optically resonant microfluidic structures, SERS integration with droplet microfluidics⁸⁴, and the optical trapping of nano-sized particles.

Optofluidic particle trapping and manipulation

Optical trapping and precise control of biological micro/nanoparticles in microfluidics improves the analytical capabilities of microsystems because the particles can be delivered to and held at the sensing/imaging locations, as opposed to relying on brief, transient interactions. For example, forces in microfluidic channels can be used to hold cells in place for imaging⁸⁵ or to focus biomolecules to the sensing region to improve the detection limit^{79, 80, 86}. In addition, plasmonic-based trapping offers the potential of the analysis of trapped particles using plasmonic sensors⁸⁷. The implementation of optofluidic techniques in combination with optofluidic sensing has led to inherently integrated methods for the analysis of biological micro- and nanoparticles in microsystems. Many of the recently reported optofluidic particle manipulation techniques and the physical mechanisms involved are described in detail in the accompanying review paper by Schmidt and Hawkins, as well as in a recent comprehensive review¹⁷. Below we describe selected applications of optofluidic micro- and nano-particle manipulation that have been demonstrated for biological applications.

The ARROW liquid core waveguide device was highlighted above for its unique optofluidic property of enabling light to propagate along a microfluidic channel with the sample. More recently, Kühn, *et al.*, have utilized the ARROW structure as a low-power optofluidic trap for small particles, including *E. coli* bacteria⁶³. As shown in Fig. 3a, light is coupled into each end of an optofluidic waveguide; due to the optical power gradient resulting from the waveguide loss, trapping forces are directed towards the longitudinal center of the channel. In addition, solid waveguides are located perpendicular and adjacent to the ARROW in order to conduct fluorescence spectroscopic analysis on trapped particles. In a later design, the authors reduced the optical power necessary for trapping to approximately 1 μ W, dramatically lower than typical optical tweezer systems⁶⁴. One could also envision a number of interesting applications for an integrated optofluidic trapping and analysis device, such as monitoring the integrity of a particular pathogenic bacterium while antibiotics are passed through the channel, or dynamically recording the binding of ligands to the receptors of a trapped biological particle.

An alternative method for creating high intensity optical power gradients for trapping in microfluidic environments is to leverage the properties of optical resonators, which can create a high intensity at the resonator surface with a decaying field extending into the fluidics. Earlier in this review, we described the use of 1-D photonic crystal resonators coupled to waveguides for RI sensing. Light of a resonant frequency forms a standing wave in the resonator with a high intensity field at the defect. Mandal, *et al.*, demonstrated the use of this resonator for the trapping of particles as small as 48 nm⁸⁸. Similarly, Arnold, *et al.*,

and Lin, *et al.*, have respectively shown that a whispering gallery mode of an optical ring resonator can trap nanoparticles and move them along the ring resonator^{89, 90}. Both of these resonator-based traps can use either RI or fluorescence mechanisms to conduct analyses of trapped particles in real time. As an example, Arnold, *et al.*, demonstrated that the microsphere carousel trap could determine the size of the trapped particle; refractive-index-based signal fluctuations caused by the radial Brownian motion of the nanoparticle reveal the radial trapping potential and thus the nanoparticle size⁸⁹.

For manipulation of larger biological particles, such as mammalian cells, laser tweezers have been the typical tool of choice. While useful combinations of laser tweezers and microfluidics have been demonstrated^{85, 91}, the systems can be cumbersome and can require high optical power. An alternative has been developed that enables the simultaneous optical control and manipulation of a large number of cells within a microfluidic chip. Chiou, *et al.*, first reported the use of a technique called optoelectronic tweezers (OET), which utilizes photocurrent-induced dielectrophoresis across a microfluidic environment (Fig. 3b)⁹². A microfluidic channel is sandwiched by an ITO layer and a photoconductive layer, while an AC voltage is applied across the two planes. Illuminating the photoconductive material converts it into a conductive electrode, and as a result, dielectrophoretic forces due to electric field gradients within the liquid medium arise. Moreover, projecting an optical image onto the photoconductive layer results in electric field gradients referenced to the illuminated areas only; this enables the dielectrophoretic control of cells in the pattern of the projected image (Fig. 3b). The authors reported the creation of 15,000 parallel traps using this approach while utilizing an optical power five orders of magnitude lower than typical optical tweezers. This technique has the potential to greatly advance the capabilities of optofluidic imaging and analysis by performing complicated steering as well as parallel and selective trapping of cells prior to analysis. One can envision the use of MEMS-based video technology to create dynamic images to perform the simultaneous trapping and complex manipulation and sorting of an unprecedented order of magnitude of cells.

Outlook

The overview presented thus far undoubtedly shows that optofluidics represents one of the most significant and active advances in the use of photonics for bio/chemical analysis. We believe that in the next five years the concept of optofluidics will be accepted by end-users outside the sensing community, and that a number of optofluidic microsystems and technologies currently under research will be commercialized to better solve actual biochemical and biomedical problems in a simpler, more cost-effective way. To take full advantage of optofluidics, we envision the following new thrusts:

- (1) *Imaging* Optofluidics has been used extensively to develop a high-resolution (sub-micron) and low-cost imaging system (or optofluidic microscope) that may replace the traditional bulky and expensive microscope^{93, 94}. It usually relies on microfluidics for sample transport, CCD/CMOS chips and masks for imaging, and post-analysis computer algorithms for reconstruction of high-resolution images. These imaging techniques have a great potential for cellular analysis in remote or resource-limited locations.
- (2) *Gas analysis*. In addition to operating on analytes in liquid, optofluidics is applicable in gas detection. One architecture is PCF that guides both gas and light along the long PCF to maximize light-analyte interaction. Both RI- and absorption-based gas detection with PCF have been demonstrated^{95, 96}. However, RI detection lacks specificity and absorption detection, while absorption, though highly specific, requires the laser to cover the wide spectral range for various gas molecules. To address those issues, recently the OFRR in

conjunction with micro-gas chromatography (μ GC) have been employed for rapid and specific gas analysis. The OFRR serves as both GC column and on-column optical gas sensor^{14, 15}, thus minimizing the number of connections and the dead volume in conventional μ GC configurations. Separation and detection of twelve gas analytes in four minutes have been demonstrated¹⁵.

- (3) Enhancement of light-matter interaction while reducing sample volume. With better photonic and microfluidic engineering, the light and sample may be confined in an extremely small volume (\sim fL), which represents a 100- to 1,000-fold decrease in the sample volume that most optofluidic devices use. Such strong interaction in a small volume may lead to detection of single molecules based on label-free or SERS detection without the need for fluorophore labeling.
- (4) *System integration using optofluidics*. The development of optofluidic systems or subsystems (rather than components) by adaptation and incorporation of other technologies in sample separation, purification, and pre-concentration, such as chromatography¹⁶, electrophoresis^{12, 13}, photophoresis⁹⁷, and nanopores⁶², will significantly enhance the bio/chemical analysis capability. Additionally, multi-modal detection involving combinations of RI, fluorescence, and SERS in the linear and non-linear regime may also be used to provide complementary information in bio/chemical analysis.
- (5) Advancement of synergies between particle control and sensing. While optofluidic particle control and sensing can be applied to detection, we envision that its largest impact will be related to bioprocess discovery at the cellular and molecular level. For example, this technique may replace the use of large laser tweezer systems that are used today for studying protein folding energy landscapes and protein binding energies.

In addition, the broad reach of optofluidics may result in unforeseen thrusts. What is clear, however, is that microfluidics research is no longer simply the miniaturization of fluidic components, while photonics-based analysis has moved beyond the goal of smaller bio/chemical sensors. Optofluidics has synergistically linked the two fields, and the result is smarter microsystems that are enabling new applications in biological and chemical analysis.

Acknowledgments

The authors wish to acknowledge the support from the National Science Foundation (ECCS-1045621 and CBET-1037097) and National Institute of Biomedical Imaging and Bioengineering (5K25EB006011).

References

1. Psaltis D, Quake SR, Yang C. Developing optofluidic technology through the fusion of microfluidics and optics. *Nature*. 2006; 442:381–386. [PubMed: 16871205]
2. Monat C, Domachuk P, Eggleton BJ. Integrated optofluidics: A new river of light. *Nature Photon*. 2007; 1:106–114.
3. Hawkins, AR.; Schmidt, H., editors. *Handbook of Optofluidics*. CRC Press; Boca Raton: 2010.
4. Fainman, Y.; Lee, L.; Psaltis, D.; Yang, C., editors. *Optofluidics: Fundamentals, Devices, and Applications*. McGraw-Hill; New York: 2010.
5. Yin D, Deamer DW, Schmidt H, Barber JP, Hawkins AR. Single-molecule detection sensitivity using planar integrated optics on a chip. *Opt. Lett*. 2006; 31:2136–2138. [PubMed: 16794704]
6. Eftekhari F, et al. Nanoholes As Nanochannels: Flow-through Plasmonic Sensing. *Anal. Chem*. 2009; 81:4308–4311. [PubMed: 19408948]

7. Huang M, Yanik AA, Chang T, Altug H. Sub-Wavelength Nanofluidics in Photonic Crystal Sensors. *Opt. Express*. 2009; 17:24224–24233. [PubMed: 20052133]
8. Guo Y, et al. Optofluidic Fabry-Pérot cavity biosensor with integrated flow-through micro-/nanochannels. *Appl. Phys. Lett.* 2011; 98:041104.
9. Galas JC, Peroz C, Kou Q, Chen Y. Microfluidic dye laser intracavity absorption. *Appl. Phys. Lett.* 2006; 89:224101.
10. Sun Y, Shopova SI, Wu C-S, Arnold S, Fan X. Bioinspired optofluidic FRET lasers via DNA scaffolds. *Proc. Natl. Sci. Acad. USA*. 2010; 107:16039–16042.
11. Sun, Y.; Fan, X. CLEO/QELS. Baltimore, MD: 2011. CWL6
12. Wang Z, Swinney K, Bornhop DJ. Attomole sensitivity for unlabeled proteins and polypeptides with on-chip capillary electrophoresis and universal detection by interferometric backscatter. *Electrophoresis*. 2003; 24:865–873. [PubMed: 12627449]
13. Zhu H, White IM, Suter JD, Zourob M, Fan X. Integrated Refractive Index Optical Ring Resonator Detector for Capillary Electrophoresis. *Anal. Chem.* 2007; 79:930–937. [PubMed: 17263318]
14. Shopova SI, et al. On-Column Micro Gas Chromatography Detection with Capillary-Based Optical Ring Resonators. *Anal. Chem.* 2008; 80:2232–2238. [PubMed: 18271605]
15. Sun Y, et al. Rapid tandem-column micro-gas chromatography based on optofluidic ring resonators with multi-point on-column detection. *Analyst*. 2010; 135:165–171. [PubMed: 20024197]
16. Lee SJ, Moskovits M. Visualizing Chromatographic Separation of Metal Ions on a Surface-Enhanced Raman Active Medium. *Nano Lett.* 2011; 11:145–150. [PubMed: 21133393]
17. Erickson D, Serey X, Chen Y-F, Mandal S. Nanomanipulation using near field photonics. *Lab Chip*. 2011; 11:995–1009. [PubMed: 21243158]
18. Pang L, Hwang GM, Slutsky B, Fainman Y. Spectral sensitivity of two-dimensional nanohole array surface plasmon polariton resonance sensor. *Appl. Phys. Lett.* 2007; 91:123112.
19. Yang J-C, Ji J, Hogle JM, Larson DN. Metallic Nanohole Arrays on Fluoropolymer Substrates as Small Label-Free Real-Time Bioprobes. *Nano Lett.* 2008; 8:2718–2724. [PubMed: 18710296]
20. Im H, Lesuffleur A, Lindquist NC, Oh S-H. Plasmonic Nanoholes in a Multichannel Microarray Format for Parallel Kinetic Assays and Differential Sensing. *Anal. Chem.* 2009; 81:2854–2859. [PubMed: 19284776]
21. Yanik AA, Huang M, Artar A, Chang T, Altug H. Integrated nanoplasmonicnanofluidic biosensors with targeted delivery of analytes. *Appl. Phys. Lett.* 2010; 96:021101.
22. Escobedo C, Brolo AG, Gordon R, Sinton D. Flow-Through vs Flow-Over: Analysis of Transport and Binding in Nanohole Array Plasmonic Biosensors. *Anal. Chem.* 2010; 82:10015–10020. [PubMed: 21080637]
23. Chow E, Grot A, Mirkarimi LW, Sigalas M, Girolami G. Ultracompact biochemical sensor built with two-dimensional photonic crystal microcavity. *Opt. Lett.* 2004; 29:1093–1095. [PubMed: 15181996]
24. Lee MR, Fauchet PM. Nanoscale microcavity sensor for single particle detection. *Opt. Lett.* 2007; 32:3284–3286. [PubMed: 18026281]
25. Lee MR, Fauchet PM. Two-dimensional silicon photonic crystal based biosensing platform for protein detection. *Opt. Express*. 2007; 15:4530–4535. [PubMed: 19532700]
26. Nunes PS, Mortensen NA, Kutter JP, Mogensen KB. Photonic crystal resonator integrated in a microfluidic system. *Opt. Lett.* 2008; 33:1623–1625. [PubMed: 18628818]
27. Mandal S, Goddard JM, Erickson D. A multiplexed optofluidic biomolecular sensor for low mass detection. *Lab Chip*. 2009; 9:2924–2932. [PubMed: 19789745]
28. Rindorf L, et al. Photonic crystal fiber long-period gratings for biochemical sensing. *Opt. Express*. 2006; 14:8224–8231. [PubMed: 19529196]
29. Huy MCP, et al. Three-hole microstructured optical fiber for efficient fiber Bragg grating refractometer. *Opt. Lett.* 2007; 32:2390–2392. [PubMed: 17700795]
30. Rindorf L, Bang O. Highly sensitive refractometer with a photonic-crystal-fiber long-period grating. *Opt. Lett.* 2008; 33:563–565. [PubMed: 18347710]
31. He Z, Zhu Y, Du H. Long-period gratings inscribed in air- and water-filled photonic crystal fiber for refractometric sensing of aqueous solution. *Appl. Phys. Lett.* 2008; 92:044105.

32. Wu DKC, Kuhlmeier BT, Eggleton BJ. Ultrasensitive photonic crystal fiber refractive index sensor. *Opt. Lett.* 2009; 34:322–324. [PubMed: 19183645]
33. White IM, Oveys H, Fan X. Liquid Core Optical Ring Resonator Sensors. *Opt. Lett.* 2006; 31:1319–1321. [PubMed: 16642098]
34. Barrios CA, et al. Label-free optical biosensing with slot-waveguides. *Opt. Lett.* 2008; 33:708–710. [PubMed: 18382525]
35. Bernardi A, et al. On-chip Si/SiO_x microtube refractometer. *Appl. Phys. Lett.* 2008; 93:094106.
36. Li H, Fan X. Characterization of sensing capability of optofluidic ring resonator biosensors. *Appl. Phys. Lett.* 2010; 97:011105.
37. Sumetsky M, Dulashko Y, Windeler RS. Optical microbubble resonator. *Opt. Lett.* 2010; 35:898–900. [PubMed: 20364162]
38. Testa G, Huang Y, Sarro PM, Zeni L, Bernini R. Integrated silicon optofluidic ring resonator. *Appl. Phys. Lett.* 2010; 97:131110.
39. Grillet C, et al. Compact tunable microfluidic interferometer. *Opt. Express.* 2004; 12:5440–5447. [PubMed: 19484104]
40. Song WZ, et al. Determination of single living cell's dry/water mass using optofluidic chip. *Appl. Phys. Lett.* 2007; 91:223902.
41. Song WZ, et al. Refractive index measurement of single living cells using on-chip Fabry-Pérot cavity. *Appl. Phys. Lett.* 2006; 89:203901.
42. Shao H, Wang W, Lana SE, Lear KL. Optofluidic Intracavity Spectroscopy of Canine Lymphoma and Lymphocytes. *IEEE Photon. Technol. Lett.* 2008; 20:493–495.
43. St-Gelais R, Masson J, Peter Y-A. All-silicon integrated Fabry-Pérot cavity for volume refractive index measurement in microfluidic systems. *Appl. Phys. Lett.* 2009; 94:243905.
44. Shumaker-Parry JS, Campbell CT. Quantitative Methods for Spatially Resolved Adsorption/Desorption Measurements in Real Time by Surface Plasmon Resonance Microscopy. *Anal. Chem.* 2004; 76:907–917. [PubMed: 14961720]
45. Ozkumur E, et al. Label-free and dynamic detection of biomolecular interactions for high-throughput microarray applications. *Proc. Natl. Sci. Acad. USA.* 2008; 105:7988–7992.
46. Vollmer F, et al. Protein detection by optical shift of a resonant microcavity. *Appl. Phys. Lett.* 2002; 80:4057–4059.
47. Zhu H, White IH, Suter JD, Zourob M, Fan X. Opto-fluidic micro-ring resonator for sensitive label-free viral detection. *Analyst.* 2008; 133:356–360. [PubMed: 18299750]
48. Ouyang H, Striemer CC, Fauchet PM. Quantitative analysis of the sensitivity of porous silicon optical biosensors. *Appl. Phys. Lett.* 2006; 88:163108.
49. Orosco MM, Pacholski C, Sailor MJ. Real-time monitoring of enzyme activity in a mesoporous silicon double layer. *Nature Nanotechnol.* 2009; 4:255–258. [PubMed: 19350037]
50. Manor R, et al. Microfabrication and characterization of Teflon AF-coated liquid core waveguide channels in silicon. *IEEE Sens. J.* 2003; 3:687–692.
51. Cho SH, Godin J, Lo Y-H. Optofluidic Waveguides in Teflon AF-Coated PDMS Microfluidic Channels. *IEEE Photon. Technol. Lett.* 2009; 21:1057–1059.
52. Korampally V, et al. Development of a Miniaturized Liquid Core Waveguide System With Nanoporous Dielectric Cladding - A Potential Biosensing Platform. *IEEE Sens. J.* 2009; 9:1711–1718.
53. Gopalakrishnan N, et al. UV patterned nanoporous solid-liquid core waveguides. *Opt. Express.* 2010; 18:12903–12908. [PubMed: 20588419]
54. Fink Y, et al. A Dielectric Omnidirectional Reflector. *Science.* 1998; 282:1679–1682. [PubMed: 9831553]
55. Ganesh N, Zhang W, Mathias PC, Cunningham BT. Enhanced fluorescence emission from quantum dots on a photonic crystal surface. *Nature Nanotechnol.* 2007; 2:515–520. [PubMed: 18654350]
56. Smolka S, Barth M, Benson O. Highly efficient fluorescence sensing with hollow core photonic crystal fibers. *Opt. Express.* 2007; 15:12783–12791. [PubMed: 19550548]

57. Coscelli E, et al. Toward A Highly Specific DNA Biosensor: PNA-Modified Suspended-Core Photonic Crystal Fibers. *IEEE J. Sel. Topics Quantum Electron.* 2010; 16:967–972.
58. Liu Y, Wang S, Park Y-S, Yin X, Zhang X. Fluorescence enhancement by a two-dimensional dielectric annular Bragg resonant cavity. *Opt. Express.* 2010; 18:25029–25034. [PubMed: 21164848]
59. Xu Q, Almeida VR, Panepucci RR, Lipson M. Experimental demonstration of guiding and confining light in nanometer-size low-refractive-index material. *Opt. Lett.* 2004; 29:1626–1628. [PubMed: 15309840]
60. Rudenko MI, et al. Ultrasensitive Q β phage analysis using fluorescence correlation spectroscopy on an optofluidic chip. *Biosens. Bioelectron.* 2009; 24:3258–3263. [PubMed: 19443207]
61. Chen A, et al. Dual-color fluorescence cross-correlation spectroscopy on a planar optofluidic chip. *Lab Chip.* 2011; 11
62. Holmes MR, et al. Micropore and nanopore fabrication in hollow antiresonant reflecting optical waveguides. *J. Micro/Nanolith. MEMS MOEMS.* 2010; 9:023004.
63. Kuhn S, et al. Loss-based optical trap for on-chip particle analysis. *Lab Chip.* 2009; 9:2212–2216. [PubMed: 19606298]
64. Kuhn S, Phillips BS, Lunt EJ, Hawkins AR, Schmidt H. Ultralow power trapping and fluorescence detection of single particles on an optofluidic chip. *Lab Chip.* 2010; 10:189–194. [PubMed: 20066246]
65. Li Z, Psaltis D. Optofluidic dye lasers. *Microfluid. Nanofluid.* 2007; 4:145–158.
66. Moskovits M. Surface roughness and the enhanced intensity of Raman scattering by molecules adsorbed on metals. *J. Chem. Phys.* 1978; 69:4159–4161.
67. Michaels AM, Nirmal M, Brus LE. Surface Enhanced Raman Spectroscopy of Individual Rhodamine 6G Molecules on Large Ag Nanocrystals. *J. Am. Chem. Soc.* 1999; 121:9932–9939.
68. Saikin SK, Chu Y, Rappoport D, Crozier KB, Aspuru-Guzik A. Separation of Electromagnetic and Chemical Contributions to Surface-Enhanced Raman Spectra on Nanoengineered Plasmonic Substrates. *J. Phys. Chem. Lett.* 2010; 1:2740–2746.
69. Nie S, Emory SR. Probing Single Molecules and Single Nanoparticles by Surface-Enhanced Raman Scattering. *Science.* 1997; 275:1102–1106. [PubMed: 9027306]
70. Kneipp K, et al. Single molecule detection using surface-enhanced Raman scattering (SERS). *Phys. Rev. Lett.* 1997; 78:1667–1670.
71. Jeanmaire DL, Duyn RPV. Surface Raman spectroelectrochemistry Part I. Heterocyclic, aromatic, and aliphatic amines adsorbed on the anodized silver electrode. *J. Electroanal. Chem.* 1977; 84:1–20.
72. Albrecht MG, Creighton JA. Anomalously intense Raman spectra of pyridine at a silver electrode. *J. Am. Chem. Soc.* 1977; 99:5215–5217.
73. Yang X, et al. High-sensitivity molecular sensing using hollow-core photonic crystal fiber and surface-enhanced Raman scattering. *J. Opt. A-Pure Appl. Op.* 2010; 27:977–985.
74. Oo MKK, Han Y, Kanka J, Sukhishvili S, Du H. Structure fits the purpose: photonic crystal fibers for evanescent-field surface-enhanced Raman spectroscopy. *Opt. Lett.* 2010; 35:466–469. [PubMed: 20160786]
75. Measor P, et al. On-chip surface-enhanced Raman scattering detection using integrated liquid-core waveguides. *Appl. Phys. Lett.* 2007; 90:211107.
76. Wang M, Jing N, Chou I-H, Cote GL, Kameoka J. An optofluidic device for surface enhanced Raman spectroscopy. *Lab Chip.* 2007; 7:630–632. [PubMed: 17476383]
77. Park S-M, Huh YS, Craighead HG, Erickson D. A method for nanofluidic device prototyping using elastomeric collapse. *Proc. Natl. Sci. Acad. USA.* 2009; 106:15549–15554.
78. Liu J, White I, DeVoe DL. Nanoparticle-Functionalized Porous Polymer Monolith Detection Elements for Surface-Enhanced Raman Scattering. *Anal. Chem.* 2011 in press, 10.1021/ac102932d.
79. Huh YS, Chung AJ, Cordovez B, Erickson D. Enhanced on-chip SERS based biomolecular detection using electrokinetically active microwells. *Lab Chip.* 2009; 9:433–439. [PubMed: 19156293]

80. Cho H, Lee B, Liu GL, Agarwal A, Lee LP. Label-free and highly sensitive biomolecular detection using SERS and electrokinetic preconcentration. *Lab Chip*. 2009; 9:3360–3363. [PubMed: 19904401]
81. White IM, Gohring J, Fan X. SERS-based detection in an optofluidic ring resonator platform. *Opt. Express*. 2007; 15:17433–17442. [PubMed: 19551037]
82. Kim, S.-m.; Zhang, W.; Cunningham, BT. Photonic crystals with SiO₂-Ag “post-cap” nanostructure coatings for surface enhanced Raman spectroscopy. *Appl. Phys. Lett.* 2008; 93:143112.
83. Choi I, Huh YS, Erickson D. Size-selective concentration and label-free characterization of protein aggregates using a Raman active nanofluidic device. *Lab Chip*. 2011; 11:632–638. [PubMed: 21120240]
84. Walter A, Marz A, Schumacher W, Rosch P, Popp J. Towards a fast, high specific and reliable discrimination of bacteria on strain level by means of SERS in a microfluidic device. *Lab Chip*. 2011; 11 10.1039/c1030lc00536c.
85. Eriksson E, et al. Optical manipulation and microfluidics for studies of single cell dynamics. *J. Opt. A-Pure Appl. Op.* 2007; 9:S113–S121.
86. Wang T-H, Peng Y, Zhang C, Wong PK, Ho C-M. Single-Molecule Tracing on a Fluidic Microchip for Quantitative Detection of Low-Abundance Nucleic Acids. *J. Am. Chem. Soc.* 2005; 127:5354–5359. [PubMed: 15826173]
87. Wang K, Schonbrun E, Steinvurzel P, Crozier KB. Scannable Plasmonic Trapping Using a Gold Stripe. *Nano Lett.* 2010; 10:3506–3511. [PubMed: 20715811]
88. Mandal S, Erickson D. Nanoscale optofluidic sensor arrays. *Opt. Express*. 2008; 16:1623–1631. [PubMed: 18542241]
89. Arnold S, et al. Whispering gallery mode carousel – a photonic mechanism for enhanced nanoparticle detection in biosensing. *Opt. Express*. 2009; 17:6230–6238. [PubMed: 19365447]
90. Lin S, Schonbrun E, Crozier K. Optical Manipulation with Planar Silicon Microring Resonators. *Nano Lett.* 2010; 10:2408–2411. [PubMed: 20545333]
91. Applegate RW, Squier J, Vestad T, Oakey J, Marr DWM. Optical trapping, manipulation, and sorting of cells and colloids in microfluidic systems with diode laser bars. *Opt. Express*. 2004; 12:4390–4398. [PubMed: 19483988]
92. Chiou PY, Ohta AT, Wu MC. Massively parallel manipulation of single cells and microparticles using optical images. *Nature*. 2005; 436:370–372. [PubMed: 16034413]
93. Cui X, et al. Lensless high-resolution on-chip optofluidic microscopes for *Caenorhabditis elegans* and cell imaging. *Proc. Natl. Sci. Acad. USA*. 2008; 105:10670–10675.
94. Bishara W, Su T-W, Coskun AF, Ozcan A. Lensfree on-chip microscopy over a wide field-of-view using pixel super-resolution. *Opt. Express*. 2010; 18:11182–11191.
95. Villatoro J, et al. Photonic crystal fiber interferometer for chemical vapor detection with high sensitivity. *Opt. Express*. 2009; 17:1447–1453. [PubMed: 19188973]
96. Cubillas AM, et al. Methane detection at 1670-nm band using a hollow-core photonic bandgap fiber and a multiline algorithm. *Opt. Express*. 2007; 15:17570–17576. [PubMed: 19551051]
97. Zhao BS, Koo Y-M, Chung DS. Separations based on the mechanical forces of light. *Anal. Chim. Acta*. 2006; 556:97–103. [PubMed: 17723334]

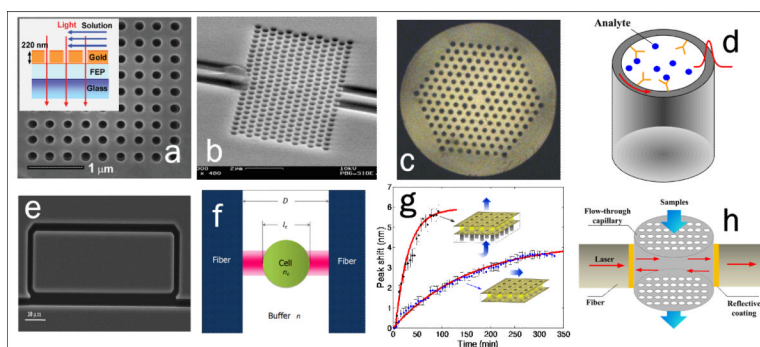


Fig. 1. Various optofluidic devices used in RI detection

a, Metallic nanohole array based plasmonic sensor¹⁹ (Reprinted with permission from American Chemical Society. Copyright 2008). **b**, Dielectric planar PC sensor²⁵ (Reprinted with permission from Optical Society of America. Copyright 2007). **c**, PCF based sensor²⁸ (Reprinted with permission from Optical Society of America. Copyright 2006). **d**, Capillary based OFRR sensor. **e**, ARROW based OFRR³⁸ (Reprinted with permission from American Institute of Physics. Copyright 2010) **f**, FP interferometric sensor for cell detection⁴⁰ (Reprinted with permission from American Institute of Physics. Copyright 2007). **g**, Flow-through vs. flow-over plasmonic sensor and the corresponding sensing response⁶ (Reprinted with permission from American Chemical Society. Copyright 2009). **h**, FP sensor with flow-through micro/nanofluidic channels⁸ (Reprinted with permission from American Institute of Physics. Copyright 2011).

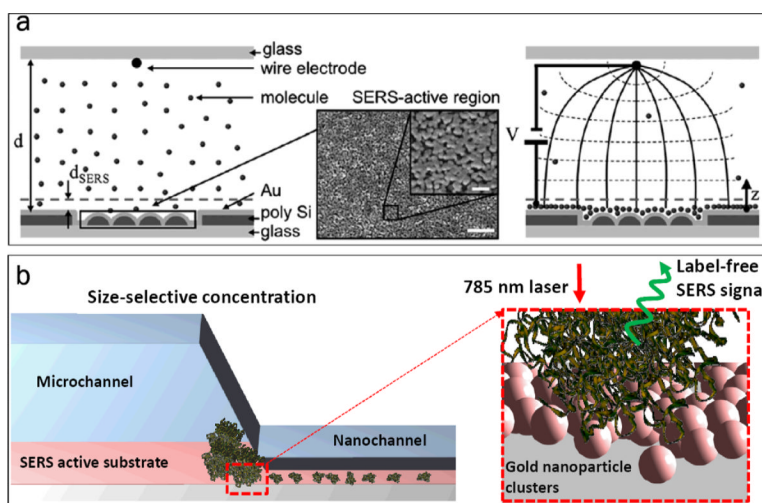


Fig. 2. Optofluidic SERS techniques

a, Electrokinetic concentration of analyte molecules at the SERS-active surface in a microchannel⁸⁰ (Reproduced by permission of The Royal Society of Chemistry). **b**, Size-selective detection of protein aggregates using a nanofluidic channel⁸³ (Reproduced by permission of The Royal Society of Chemistry).

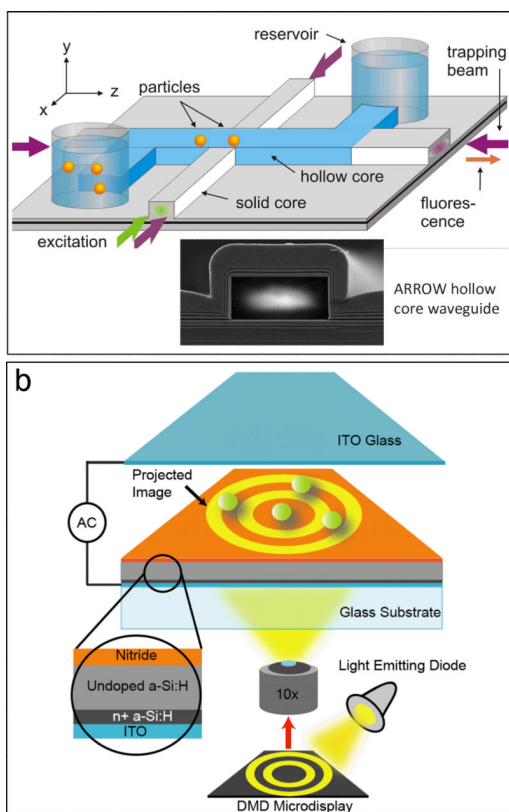


Fig. 3. Various optofluidic devices for nanoparticle trapping and manipulation
a, Particle trapping and fluorescence analysis using a liquid core ARROW waveguide structure⁶³ (Reproduced by permission of The Royal Society of Chemistry). **b**, Optoelectronic tweezers for the parallel control of cells in a microfluidic channel⁹² (Reprinted by permission from Macmillan Publishers Ltd: Nature copyright 2005).